NASA-CR-193305

IN-39-CR
175472
P.41

SIMULATION STUDIES FOR SURFACES AND MATERIALS STRENGTH

Semiannual Progress Report

for
Cooperative Agreement NCC2-297

for the period
November 1, 1992 - April 30, 1993

Submitted to

National Aeronautics and Space Administration
Ames Research Center
Moffett Field, CA 94035

Computational Chemistry Branch
Dr. Steve Langhoff, Chief

Thermosciences Division
Dr. Jim Arnold, Chief

Prepared by
Eloret Institute
1178 Maraschino Drive
Sunnyvale, CA 94087
Phone: 408 730-8422 and 415 493-4710
K. Heinemann, President and Grant Administrator
Timur Halicioglu, Principal Investigator

N94-13179
Unclas
G3/39 0175472
(NASA-CR-193305) SIMULATION STUDIES FOR SURFACES AND MATERIALS STRENGTH Semiannual Progress Report, 1 Nov. 1992 - 30 Apr. 1993 (Eloret Corp.) 47 p

During this period investigations were carried out in three areas:

1. Optimum energies and structures were estimated for single step ledges formed on the (111) surface of diamond. Calculations were carried out employing a recently developed model potential function for carbon species. Four different ledge combinations along the close packed direction were investigated and variations in excess ledge energies were reported as a function of ledge-ledge separation. In general, interactions between ledges were found to be operational up to separations corresponding to 4 surface lattice spacings. The excess energy for the ledge in the $[\bar{2}11]$ outward normal direction with an *upper* dangling atom, is the highest among the other ledge structures included in this work. Calculations carried out in this study indicate that relaxed stuctures of ledges formed on the diamond (111) surface are different from the corresponding ledge structures on the Si(111) surface. Computational details along with a short discussion of the results are presented in Appendix I.

2. Binding energies of carbon atoms adsorbed on a (2×1) reconstructed Si(100) surface were calculated as a function of sub-monolayer coverages. Also calculated were energies for carbon atoms deposited on the surface as small clusters, C_n, (with n=2 and 3). All calculations were conducted considering a model potential function developed recently for systems containing C and Si atoms. For the low coverage limit, (representing coverages up to one monolayer) carbon adatoms were considered as occupying only low energy surface sites. Due to relatively large separations among these sites,

C-C interactions are negligible and Si-C interactions are found to be contributing to binding energies. The lowest binding energy in this case corresponds to a coverage of θ=0.25. Small carbon clusters deposited on the surface, however, were found to be energetically more stable. From an energetic viewpoint results obtained in this study indicate that adsorbing C atoms on a Si(100) surface are more likely to form clusters than a smooth and uniform surface coverage. Details of this investigation are presented in Appendix II.

3. In this part, calculations were conducted to analyze the strain dependence of the binding energy of a carbon adatom deposited on a (2×1) dimerized Si(100) surface. Two different low energy binding sites on the reconstructed Si(100) surface were taken into consideration. The lowest energy site is located near the top position of a second layer Si atom; while the second lowest energy site is at the bridge site between two top layer Si atoms forming the dimer. Results indicate that the binding energy for a carbon atom adsorbed in the lowest energy sites is affected most by the external strain. In particular, the effect of an uniaxial strain applied in the direction perpendicular to the surface Si-dimers, was found to be quite significant. While a tensile stress in this direction produces an increase in the value of the binding energy, a compressive strain was found to lower the binding energy. In general, strains applied in the direction parallel and perpendicular to Si-dimers were found to produce opposing effects on the binding energies. This study is still in progress, results obtained during this period are summarized in Appendix III.

APPENDIX I:

Calculations for Ledge Energies on the Diamond (111) Surface

Introduction

An atomic level understanding of surface defects is highly desired by surface scientists today. It has been well recognized that in many surface related processes the role played by surface defects is important [1,2]. Despite the fact that significant progress has been made on experimental techniques for the growth of diamond [3], the dependence of the properties of the growing film on the local surface structure is not yet well understood. In order to analyze fully many-nested processes taking place in or around defective regions during the film growth, an atomic level understanding of surface defects is needed.

In this study, simulation calculations were performed to investigate microscopic properties for single step ledges formed on a diamond (111) surface. In addition to local structures, excess energies for ledges were also calculated for varying ledge-ledge separations. Investigations were carried out at an atomic level using an energy minimization technique based on a model potential function developed recently by Tersoff for carbon species. The Tersoff function has 11 adjustable parameters and it describes accurately many properties of the diamond crystal as well as properties of an individual graphitic plane [4]. More recently it has also been employed in calculating surface properties for the low index plane of diamond [5].

Calculations

In the present investigation, the (111) surface was first generated as an abrupt termination of a properly oriented diamond crystal with a lattice constant of 3.5656 Å in a diamond cubic structure. This lattice separation corresponds to the minimum energy configuration of an ideal

diamond crystal calculated by the Tersoff function [4]. A side view of the atomic positions in the several top layers of the (111) surface (for an unrelaxed ideal case) is depicted in Figure 1. The atomic layers in this case come in pairs, and are best considered as puckered layers of *upper* and *lower* atoms [6]. While the inter-layer spacing, δ, represents the separation between the *upper* and *lower* atoms of the same puckered layer, the intra-layer spacing, Δ, is the distance between two successive puckered layers as shown in Figure 1. For an unrelaxed case, the inter-layer spacing is just one third of the intra-layer spacing which is equal to the nearest neighbor distance in the ideal diamond lattice [6]. Upon relaxation, however, both inter- and intra-layer spacings in the exposed surface region exhibit large variations [5].

Simulation runs were carried out considering computational cells with varying dimensions containing up to 800 carbon atoms, depending on the system size and the type of the ledges. Throughout this study computational cell dimensions were represented by L_x, L_y and L_z corresponding to the three cartesian directions x, y and z, respectively. In generating surfaces, periodic boundary conditions were imposed on the system along the x and y directions (parallel to the exposed surface) in order to provide continuity. Accordingly, two surfaces were left exposed in the direction perpendicular to the z axis. Computational cells contained at least 6 puckered layers (i.e., a total of 12 *upper* and *lower* atomic layers) parallel to the surfaces. In order to investigate the size dependence of the energy- and structure-dependent properties, we repeated calculations for a few selected cases, considering more atomic layers. In all cases they produced virtually identical results.

The total potential energy of a system of N particles is described

as:

$$E = \sum_{i}^{N} \Phi_i \tag{1}$$

where Φ_i denotes the energy per atom calculated by the Tersoff function. To obtain relaxed configurations, the total energy of the system was minimized with respect to the positions of all atoms in the computational cell. First the energy, γ_s, of a defect-free surface was calculated as:

$$\gamma_s = \frac{E_s - E_b}{A} \tag{2}$$

where E_b denotes the total relaxed energy for the bulk with no surface and E_s is the total relaxed energy of the same system with surfaces. The total area of the exposed surface is denoted by A and it is equal to $2 \times L_x \times L_y$.

Ledges were created on the (111) surface by simply removing a number of carbon atoms from the top puckered layer. All ledges in the top surface layer were formed parallel to the $[01\bar{1}]$ direction (which is the close-packed direction). The ledge energies in the $[01\bar{1}]$ direction were found to be the lowest among the energies for ledges created in other low index directions on the (111) surface. In each case, two opposing ledges were created on the surface within the computational cell. A macroscopic view of the system obtained by stacking four computational cells in the y direction is shown in Figure 2. In all cases, the lower and higher terraces were formed to have approximately equal areas.

On the (111) surface, four different ledge structures are possible along the $[01\bar{1}]$ direction. Each ledge is different according to its outward normal direction (either $[\bar{2}11]$ or $[2\bar{1}\bar{1}]$) and whether it terminates on a row of *upper* or *lower* atoms. For an unrelaxed system in the outward $[\bar{2}11]$ direction an *upper* atom has only one neighbor located in the lower

layer and a *lower* atom in the same outward direction has two neighbors which are located in the upper layer. On the other hand, in the outward $[2\bar{1}\bar{1}]$ direction an *upper* atom has two neighbors located in the lower layer and a *lower* atom has only one neighbor in the upper layer [6]. Schematic side views for the four opposing ledge combinations which are included in this study, are shown in Figure 3 for unrelaxed cases. These structures were denoted by A1, A2 and S1, S2, representing asymmmetrical and symmetrical configurations for opposing ledges. The ledge-ledge distance, d_L, (basically measuring the ledge spacing along the lower terrace) was varied by increments (m) of a_i which denotes the surface lattice spacing in the direction perpendicular to the ledges. Calculations were carried out for $d_L = m \times a_i$ with varying values of m from 2 to 6.

The excess ledge energy, γ_l, per unit length was calculated as:

$$\gamma_l = \frac{E_l - E_b - 2L_x L_y \gamma_s}{D} \tag{3}$$

where E_l is the total energy of the system bearing ledges with a total length of D. The two dimensions of the computational cell describing the exposed surface area are denoted by L_x and L_y. Relaxed values of γ_l were calculated using two different initial configurations. The ledges were created using (i) relaxed and (ii) unrelaxed defect-free surfaces. In both cases, however, the system was fully equilibrated after the formation of the ledge to obtain the relaxed ledge energy value. In general, we obtained identical values. In some cases however, for the two different initial configurations, slightly different values of γ_l were obtained. For those cases, only the lower values were considered.

Results and Discussion

For a defect-free (111) plane of diamond the unrelaxed and fully-relaxed surface energies were calculated as 4045 and 2744 ergs/cm^2, respectively. These values of γ_s, as well as structural changes at the exposed surface due to the multilayer relaxations, were found to be consistent with an earlier calculation carried out for the T=100 K case [5]. Calculated excess energies for varying ledge-ledge separations are given in Table 1 for four different equilibrated ledge structures. Also, Figure 4 shows variations in calculated ledge energies as functions of ledge spacings. The values of γ_l calculated here, represent average values for two opposing relaxed ledges with outward normal directions of $[\bar{2}11]$ and $[2\bar{1}\bar{1}]$ as shown in Figure 3.

Results indicate that excess energies for ledges on the (111) surface of diamond, exhibit relatively little dependence on the ledge spacings. In general, ledge energies calculated for A1 and S1 structures were found to be smaller than the values obtained for A2 and S2 cases. The A1 structure has a ledge with a *lower* atom in the outward $[\bar{2}11]$ direction opposing a ledge with an *upper* atom in the outward $[2\bar{1}\bar{1}]$ direction. The effect of the ledge spacing in this case is noticeable between m=3 and m=4, where the calculated value of γ_l decreases about 0.2 eV/Å. For the S1 structure, both ledges terminate with *lower* atoms. (See Figure 3). In this case, the variation of the ledge energy as a function of ledge-ledge separation is more pronounced. The calculated value for γ_l was found to be first decreasing for the m=3 spacing. It then increases for m=4 before it plateaus for m=5 and 6 spacings. For the A2 structure we have one ledge in the outward $[\bar{2}11]$ direction with an *upper* atom facing another ledge in the outward $[2\bar{1}\bar{1}]$ direction terminated by a *lower* atom. Calculations in this case produced only a small decrease in the

value of γ_l for the m=3 spacing. Ledge energies calculated for the S2 structure (with both ledges terminating with *upper* atoms) exhibit almost no dependence on the ledge spacing.

An analysis of the present results indicates that the excess energy is the lowest for a ledge with a *lower* atom in the outward [$\bar{2}$11] direction. On the other hand, a ledge with an *upper* atom in the same outward direction has the highest excess energy.

In general, for larger ledge spacings the displacement of atoms upon relaxation was found to be rather minimal in the vicinity of ledges as well as on the terrace regions. The relaxed structure for the S1 type ledge combination (which produced the lowest energy for the $m = 3$ case) is schematically shown in Figure 5. In this case, the relaxation takes place basically in the upper terrace. The geometry of the upper terrace is changed as a result of a ''pop-up" relaxation mechanism (which has been described in reference 6 for the Si case). Upon relaxation each lower atom located in the middle section of the upper terrace moves upward, popping up through the triangle of its three upper neighbors. The bonds between the pop-up atom and its upper neighbors are not broken, but, they are simply everted through the surface plane [6].

Both A2 and S2 structures have dangling *upper* atoms in the outward [$\bar{2}$11] direction. Upon relaxation, the local structure around these ledges was virtually unchanged and the *upper* atoms remained upward. This result is somewhat different from the relaxed ledge structures reported for the (111) surface of Si [6,7]. In the case of Si, the *upper* dangling atom for a ledge in the outward [$\bar{2}$11] direction has been found to bend downward, approaching the lower terrace upon relaxation [6]. This is shown schematically in Figure 6. For a better comparison, we used one of the recent Tersoff potential functions [8] for Si and investigated re-

laxation features of the same ledge (with an *upper* Si atom in the outward [$\bar{2}11$] direction). After relaxation the *upper* dangling atom was found to have moved downward (as shown in Figure 6) and the relaxed structure was almost identical with findings reported by Pearson [6]. Several attempts were made in this study to find a minimum energy structure analogous to the Si case for the same ledge formed on the (111) surface of diamond (in the outward [$\bar{2}11$] direction terminating with an *upper* carbon atom). Calculations were carried out for the diamond case with different initial configurations (including a bent down dangling atom configuration). However, no minimium energy structure was found similar to the Si case with a bentdown dangling atom.

Another structural difference between the ledges formed on the (111) surfaces of diamond and of silicon that was found in this study, concerns the formation of dimers along the ledges. In the case of Si, our calculations produced dimers (upon relaxation) along the ledge in the outward [$\bar{2}11$] normal direction terminating with *upper* atoms as well as along the ledge in the outward [$2\bar{1}\bar{1}$] normal direction terminating with *lower* atoms. These results are consistent with earlier reports on dimer formations along ledges formed on the Si(111) surface [6,7]. In the present investigation, however, no dimer formation was found along these ledges for the diamond case. In fact, even in calculations performed with intially dimerized ledge structures, dimers were undone during the relaxation and after a complete equilibration, no dimer structures were found.

Conclusions

Ledges formed on the (111) surface of diamond were found to display virtually no long range ledge-ledge interactions for separations larger

than four surface lattice spacings. Ledge combinations of A1, A2, and S1 types exhibited some ledge-ledge interactions for separations corresponding to 3-4 surface lattice spacings, while for the S2 type ledge combination, no intra-ledge interactions were found for separations up to $m = 6$. For the S1 type ledge combination the excess ledge energy was found to be reduced further due to a ''pop up" relaxation mechanism. Present calculations for A1- and S1-type ledge combinations produced lower excess energies; accordingly, these ledges are more likely to be found on the (111) surface of diamond. It was also found that the excess energy for the ledge in the $[\bar{2}11]$ outward normal direction with an *upper* dangling atom, was higher than other ledge structures included in this work. Calculations carried out in this study produced somewhat different relaxed ledge stuctures for the diamond (111) surface than the ledge structures reported for the Si case.

References

[1] K. Wandelt, Surf. Sci., 251/252 (1991) 387.

[2] V. Bortolani, N. H. March and M. P. Tosi (eds), *Interaction of Atoms and Molecules with Solid Surfaces*, Plenum Press, New York, 1990.

[3] H. Shiomi, K. Tanabe, Y. Nishibayashi and N. Fujimori, Jpn, J. Appl. Phys., 29 (1990) 34.

[4] J. Tersoff, Phys. Rev. Lett., 61 (1988) 2879.

[5] T. Halicioglu, Surf. Sci., 259 (1991) L714.

[6] E. M. Pearson, *Computer Modeling of Atomic Interactions with Application to Silicon*, 1985. Ph.D. Thesis, Department of Materials Science and Engineering, Stanford University.

[7] D. J. Chadi and J. R. Chelikowsky, Phys. Rev. B, 24 (1981) 4892.

[8] J. Tersoff, Phys. Rev. B, 39 (1989) 5566.

Table 1. Calculated excess ledge energies (in eV/Å) for varying ledge-ledge separations given in multiples (m) of the surface lattice spacing.

$m =$	2	3	4	5	6
A1	0.564	0.566	0.351	0.349	0.349
A2	1.214	1.184	0.961	1.102	1.102
S1	0.547	0.195	0.631	0.416	0.416
S2	1.249	1.249	1.249	1.249	1.249

Figure Captions

1. A schematic side view of atomic positions in the top layers of the diamond (111) surface. The inter-layer spacing is denoted by δ_i representing the separation between the *upper* and *lower* atoms of the same puckered layer. The distance between two successive puckered layers is denoted by Δ_i.

2. A macroscopic view of the ledges obtained by stacking four computational cells in the y-direction. Calculations were carried out considering periodic boundary conditions (PBC) in x- and y-directions. Computational cell dimensions were represented by L_x, L_y and L_z corresponding to the three cartesian directions.

3. Schematic side views for different ledge combinations. Opposing ledges terminating with a row of *upper* or *lower* atoms are shown in $[\bar{2}11]$ and $[2\bar{1}\bar{1}]$ outward directions as indicated by arrows. Asymmetrical and symmetrical configurations with respect to *upper* or *lower* atoms are labeled by A1, A2 and S1, S2.

4. Variations in excess ledge energies for A1, A2 and S1, S2 combinations as a function of ledge-ledge distance (which is shown in multiples of the surface lattice spacing).

5. A schematic side view for the relaxed S1 ledge configuration at a separation of $3a$ (where, a is the surface lattice spacing in the direction perpendicular to the ledge). The dotted line shows the elongated C-C bond between the "pop-up" atom and its neighbor in the layer below.

6. A side view for a ledge in the outward [$\bar{2}11$] direction with an *upper* atom. In the case of diamond the position of the *upper* atom remains virtually unchanged upon relaxation. For the Si case, however, relaxation causes the *upper* atom to move downward as indicated by the arrow.

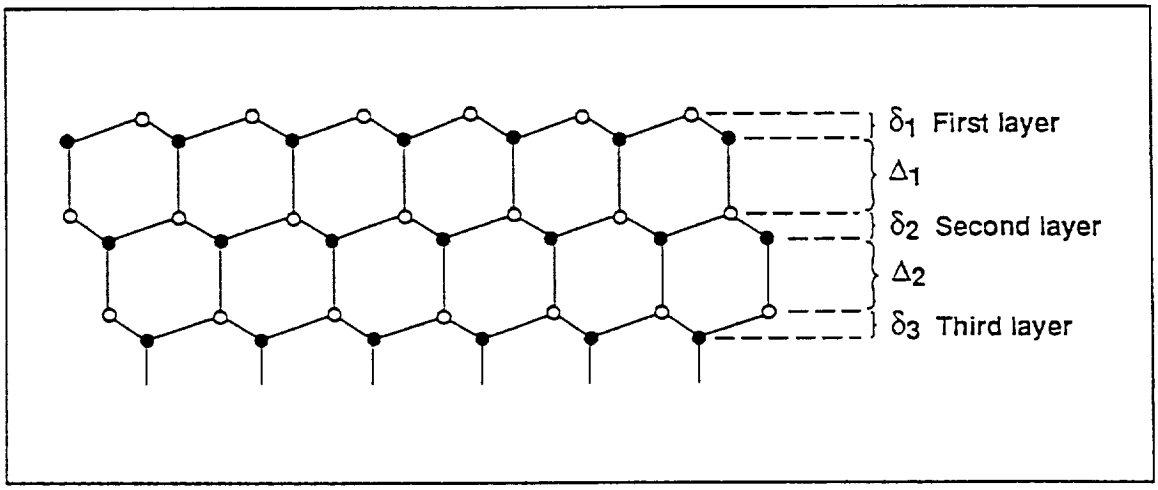

Figure 1

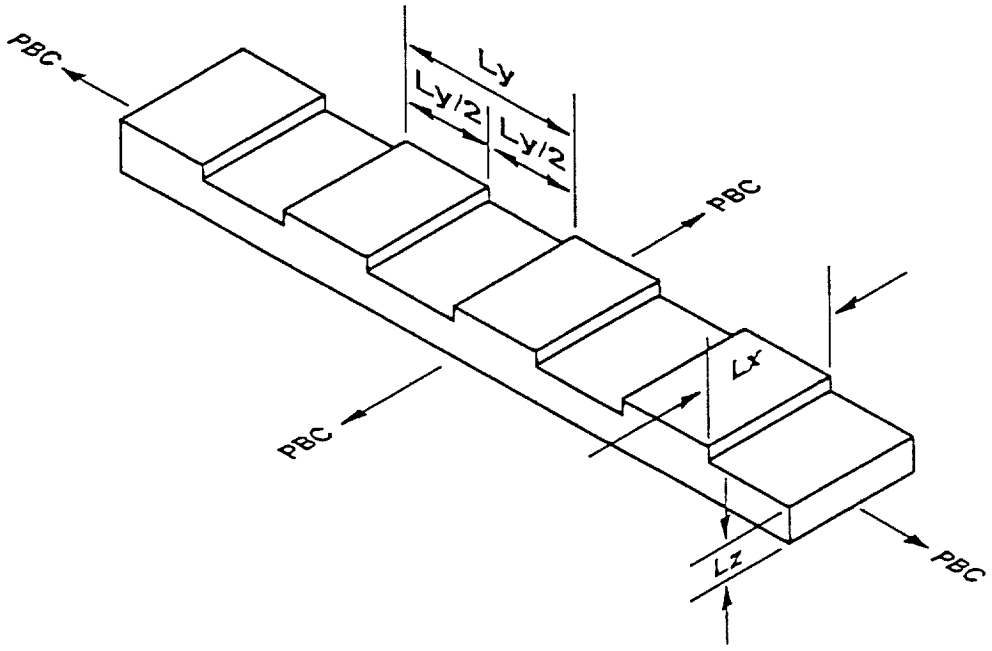

Figure 2

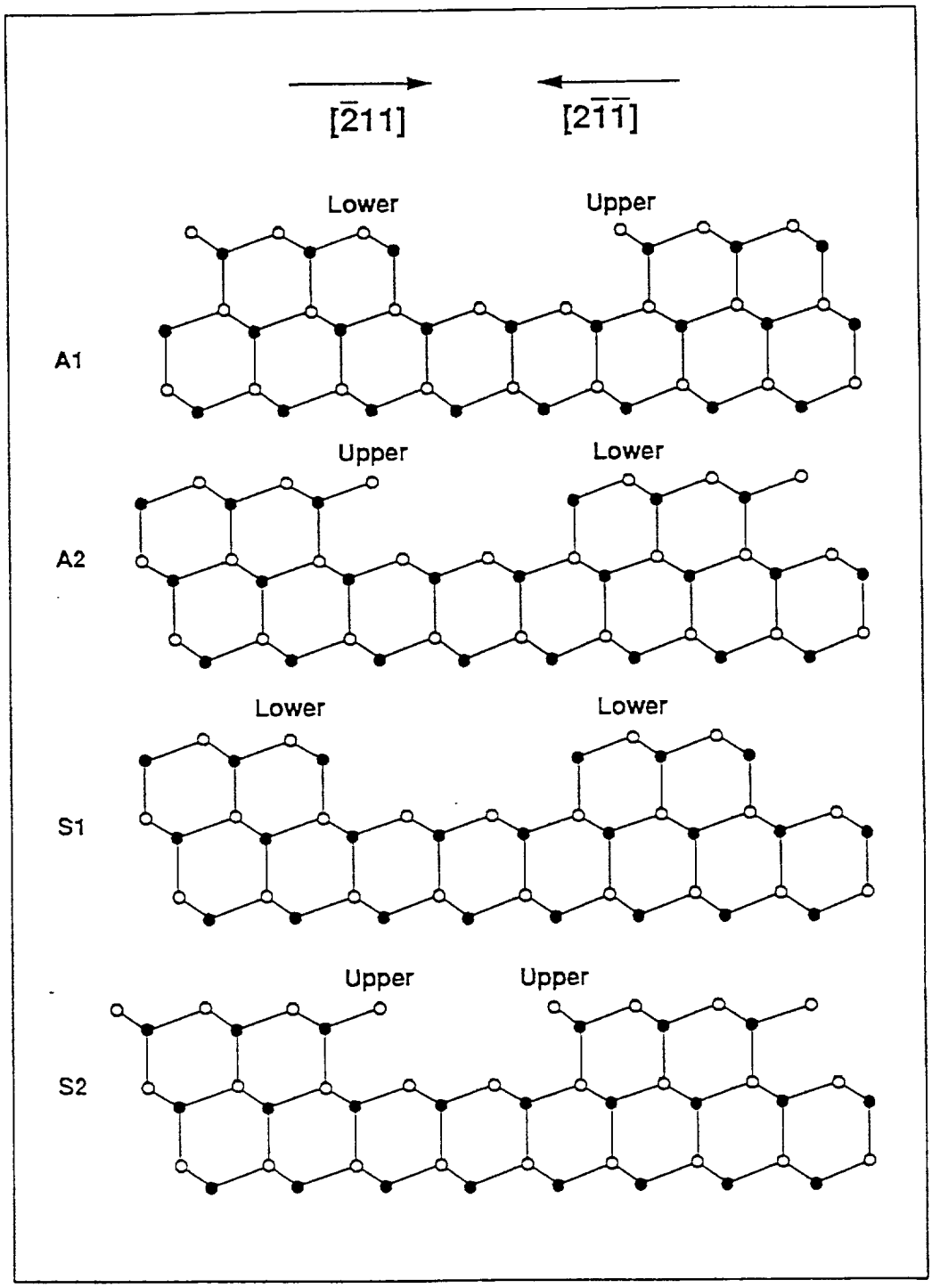
[$\bar{2}11$]
[$2\bar{1}\bar{1}$]
Lower
Upper
A1
Upper
Lower
A2
Lower
Lower
S1
Upper
Upper
S2

Figure 3

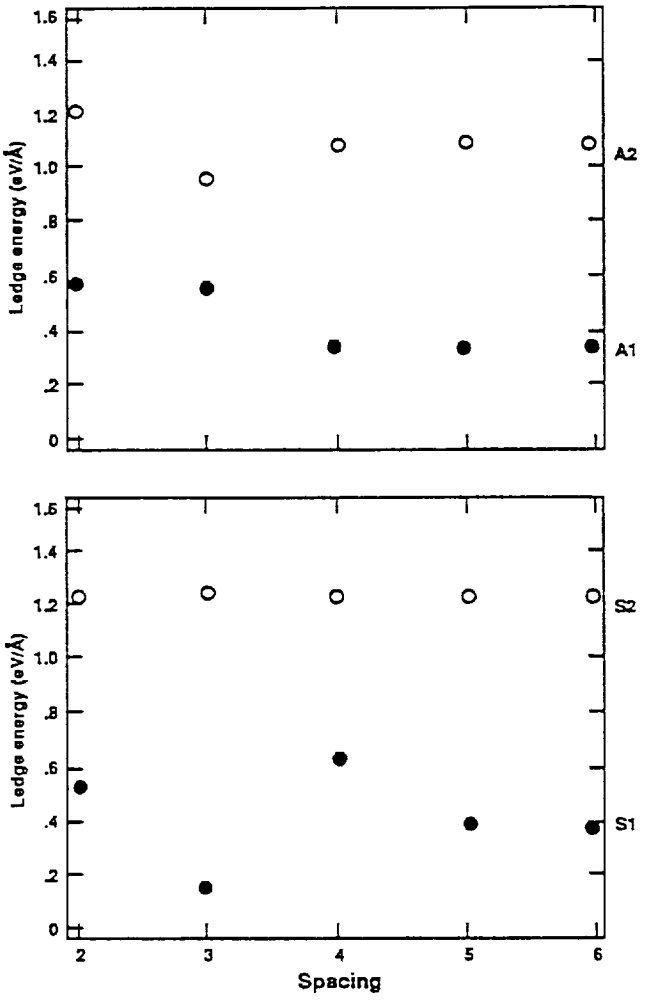

Figure 4

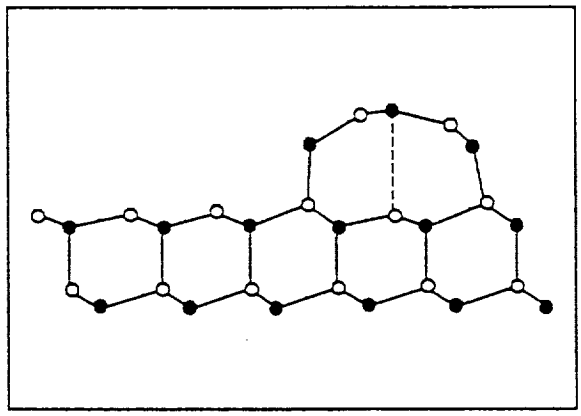

Figure 5

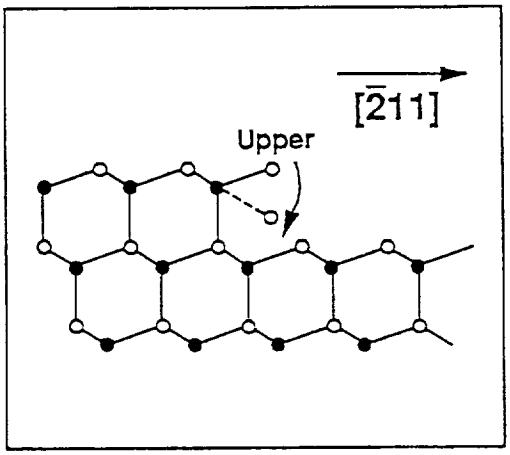

Figure 6

APPENDIX II:

Binding Energies for Carbon Adatoms and Clusters Deposited on the Si(100) Surface

Introduction

Binding energies for adatoms and their dependence on the surface coverage represent an important feature in the analysis of the early stages of the surface deposition process. In the case of diamond film synthesis, for instance, many nucleation as well as growth characteristics were found to be dependent on the structure of the substrate surface and on its coverage state [1-3].

In this investigation calculations were performed, first, to estimate binding energies of carbon atoms distributed uniformly on a (2×1) dimerized Si(100) surface as a function of the surface coverage. Binding energies along with the locations of the energetically favorable adsorptions sites for one and two carbon adatoms deposited on a Si(100) surface, have been determined recently [4]. Here, a similar calculation procedure was employed and binding energies were calculated for carbon adatoms (distributed uniformly over the avalaible low energy sites) forming a monolayer or sub-monolayer structure on the surface region. In the second part of this study, calculations were carried out to estimate energies for small clusters of carbon atoms formed on the Si(100) surface.

In calculating energies in this study a model potential function developed by Tersoff [5] (specifically for systems containing Si and C atoms) was used throughout. This function has been employed recently in calculating energies for carbon defects formed on the reconstructed Si(100) surface [4]. The same analytic function, with a small change of parameters for C, has also been used in calculating energies and structures for carbon defects in bulk Si [6]. At the same time, it has been shown that for pure Si systems also, the Tersoff function produces ac-

ceptable results for various bulk and surface properties [7]. Furthermore, for pure carbon systems this function is able to reproduce correctly many bulk properties of diamond and of the graphitic plane, and recently it has been used to estimate surface properties for low index planes of diamond [8].

Method of Calculation

The Si(100) surface was first considered as an abrupt termination of bulk silicon in the diamond cubic structure with a lattice constant corresponding to the equilibrium volume of Si calculated by the Tersoff function. Then, the system was equilibrated producing (2×1) dimerized reconstruction patterns at the exposed (100) surface. In the equilibration process, every atom in the system was permitted to relax by minimizing the total energy with respect to the atomic coordinates. Throughout this study, periodic boundary conditions were imposed on the system in two directions (parallel to the exposed surface) in order to provide continuity. Simulation calculations were carried out considering a 4×4 computational cell which was made of a slab of 16 atomic layers, each containing 16 Si atoms. This cell size was found to be adequate for the convergence of the defect-free surface energy [4].

In all cases, binding energies, ϕ_b, per carbon adatom were calculated as:

$$\phi_b = \frac{1}{m}[E_a^{(m)} - E^o] \tag{1}$$

where m is the number of adatoms, E^o denotes the total equilibrated energy of the system of N particles with clean exposed surfaces, and $E_a^{(m)}$ is the total relaxed energy of the same system with m adatoms deposited on the surface.

In this study, monolayer and sub-monolayer coverages were first investigated considering a uniform carbon atom distribution. On a fully relaxed Si(100) surface, carbon atoms were positioned at the lowest energy sites and binding energies for varying coverages were calculated after a full reequilibration of the system. In an earlier study it has been shown that for a carbon adatom the lowest energy site at this surface is located near the top position of a second layer Si atom [4]. In Figure 1 which depicts the top view of a clean dimerized Si(100) surface, identical low energy binding sites for C atoms are indicated by letters a through p.

Results and Discussions

Calculations were performed for six different coverages and the results are presented in Table 1. A full coverage in this study is defined as $\theta = 1$, when all the low energy sites at the surface are occupied by carbon atoms. This is denoted as structure number 1 in Table 1. For this case calculations produced a relatively high binding energy for C adatoms, contrary to expectations. Here, carbon atoms form a perfect two-dimensional layer and each carbon atom is located within the top Si layer as has been shown in reference [4].

For a coverage corresponding to $\theta = 3/4$, three different C adatom arrangements were considered at the exposed surface. For structure number 2, binding sites located in three adjacent rows (which run parallel to the Si-dimers) were occupied by carbon atoms. This configuration corresponds to the most favorable structure for a 3/4 coverage. For structure number 4, on the other hand, the binding energy per atom is about 0.414 eV higher than the energy calculated for structure number 2. In this case, the three adjacent rows which were occupied by carbon atoms, are

perpendicular to Si-dimers. For structure number 3, as indicated in Table 1, four sites in the diagonal direction were left unoccupied. This produced an intermediate binding energy value, as anticipated.

For $\theta = 1/2$, five different configurations were taken into consideration. The lowest binding energy was calculated for tstructure number 5. In this case, two adjacent rows of low energy sites which run parallel to Si-dimers, are occupied by carbon atoms. On the other hand, for carbon atoms positioned in alternating rows parallel to Si-dimers calculations produced the second lowest binding energy (see Table 1, structure number 5) which is about 0.19 eV higher than the binding energy for structure 5. In the case of structures 7, 8 and 9 (where, carbon atoms were deposited in alternating diagonal rows, in alternating rows perpendicular to Si-dimers and in two adjacent rows perpendicular to Si-dimers, respectively) calculations produced approximately similar binding energy values which were all found to be about 0.38 eV higher than the energy calculated for structure number 5.

For a coverage corresponding to $\theta = 1/4$, calculations were performed for four different deposition patterns. The strongest binding was found for carbon adatoms occupying a row of sites aligned parallel to Si-dimers. This is shown in Table 1 as structure number 10. The weakest binding, on the other hand, corresponds to structure 13, where C adatoms are positioned in a row perpedicular to Si-dimers. Carbon adatoms occupying alternating sites in both parallel and perpendicular directions to Si-dimer (see Table 1, structure number 12) produced a somewhat stronger binding which is about 0.09 eV lower than the binding energy for the structure number 13. Finally, for carbon atoms deposited on the neighboring four sites forming a square (structure number 11), the binding energy per carbon atom was found to be only 0.019 eV higher

than the energy of structure 10.

For the case $\theta = 1/8$, seven different configurations were taken into consideration. These are shown in Table 1 (structures numbered 14 through 20). The strongest binding was calculated for structure number 14, where carbon atoms occupy two neighboring sites in the direction parallel to Si-dimers. The second strongest binding was obtained for structure number 15, corresponding to carbon atoms occupying two neighboring sites in the direction perpendicular to Si-dimers. In this case the binding energy is only 0.047 eV higher than the energy of structure 18. Other configurations for the $\theta = 1/8$ case produced somewhat higher binding energies as tabulated in Table 1. The weakest binding was calculated for structure number 20, corresponding to carbon atoms occupying two alternating sites on a row perpendicular to Si-dimers.

For a coverage of $\theta = 1/16$, the binding energy per C atom is shown in Table 1 as structure number 21. In this case, only one carbon atom was located on the (4×4) surface.

In general, deposited C atoms upon relaxation remain in the close proximity of their lowest energy binding sites. However, only for in the case of structure 4, carbon atoms located at sites c, g, k, o were found to be displaced for about 0.5 Å toward the empty sites d, h, l, p during the equilibration procedure.

Figure 2 displays the lowest binding energy values (for different θ's from Table 1) plotted against the surface coverage. The carbon adatom binding energy up to a single monolayer is the most favorable for a coverage corresponding to $\theta = 1/4$. In monolayer or sub-monolayer coverages of carbon atoms on the Si(100) surface (as considered above, for C atoms located at the lowest energy sites) the closest C-C distance is

3.70 Å. This separation is well beyond the cutoff region of the Tersoff function. Therefore, binding energies calculated above for dilute and uniformly distributed carbon atoms do not contain any direct contributions coming from the C-C interactions. All the binding energies are due purely to Si-C interactions. It is believed that variations in binding energies are primarily the result of stress effect. This situation, corresponding to a dilute and uniform carbon atom distribution on the surface, should rather be regarded as a limiting case respresenting perhaps the very early stages of the deposition process.

For a non-uniform carbon atom distribution on the surface, however, carbon clusters are expected to form in regions of high C atom concentrations. In such cases, C-C distances are shorter and, therefore, interactions among carbon atoms contribute to binding energies (as defined by Eq. 1). Next, calculations were performed to estimate the average binding energies for small carbon clusters, C_n (with $n = 3$ and 4), deposited on a fully relaxed Si(100) surface. For each case, we used over 15 different initial configurations considering different atomic positions for clusters and varying adsorption sites on the surface. The top and side views of the energetically most favorable structure for C_3 on a Si(100) surface are shown schematically in Figure 3. In this case, C_3 forms an obtuse triangle lying in a plane perpendicular to the exposed surface and at the same time it is perpendicular to Si-dimers. For the equilibrated configuration, calculated values for the apex angle and distances are shown in Figure 3. The three carbon atoms are symmetrically situated between two Si-dimers and the carbon atom in the middle is exactly above the third layer Si atom. The middle C atom protrudes and it is situated about 1.37 Å above the surface plane (passing through the four neighboring Si atoms forming the dimers). The distance between an end-carbon atom of C_3 and a Si atom of the nearest dimer is 1.871 Å.

There are four such distances as shown in Figure 3. The binding energy in this case was calculated as -6.7993 eV which is about 0.43 eV lower than the energy corresponding to a coverage of $\theta = 1/4$.

For C_4 the fully relaxed structure corresponding to the lowest-lying state is shown in Figure 4. In this case also, the cluster is symmetrically located between two Si-dimers, and carbon atoms form a planar trapezoid which is perpendicular to the surface plane and to Si-dimers (somewhat similar to the C_3 case). The distance between the two top carbon atoms which protrude from the surface, was calculated as 1.449 Å. They were found to be about 2.1 Å above the surface plane. The two lower carbon atoms of the cluster (forming the base of the trapezoid) on the other hand, are only 0.88 Å above the surface plane. The C-C-C angle along with distances among C and Si atoms for the adsorbed C_4 cluster are indicated in Figure 4. The binding energy, in this case, was calculated as -6.5625 eV. While this is somewhat higher than the C_3 case, it is still energetically more favorable than the sub-monolayer coverage of $\theta = 1/4$.

Results obtained here indicate that clustering of C adatoms at the surface is energetically favorable. This conclusion is, of course, based on the static approximation employed here. No attempt was made to estimate diffusivities of carbon adatoms on the surface in the process of forming clusters via surface migrations. In this relatively simple simulation calculation we considered only a system containing C and Si atoms. Other elemental or molecular species (like H, CH_4, etc.) often used in diamond growth experiments were not included. From a purely energetic viewpoint, the present investigation suggests that adsorbing carbon atoms on a Si(100) surface are more likely to form small clusters than a uniform monolayer coverage. To some degree this outcome is con-

sistent with various experimental findings that ''scratching", which leaves carbonaceous materials on a Si(100) surface, plays an essential role in promoting the nucleation process [1,9,10]. Furthermore, in genaral, a layer-by-layer growth mechanism has not been observed in diamond film experiments.

Conclusions

Calculations were carried out to estimate binding energies for carbon atoms adsorbed on a reconstructed Si(100) surface. For submonolayer coverages (considering that carbon atoms are located on the periodic low energy binding sites on the surface) the lowest binding energy corresponds to a coverage of $\theta = 1/4$. In this case, distances between carbon atoms are large and calculated binding energies have no contributions coming from the C-C interactions.

For small clusters of carbon (C_n, with n=3 and 4) adsorbed on the surface, however, interactions among the carbon atoms reduce the total binding energy further and make the clusters energetically more favorable. In their relaxed configurations the clusters on the surface were not flat, but rather were found to be protruding. The presence of carbon atoms clustered in the surface, promotes formation of stronger binding sites (in the contiguous region) for the incoming carbon atoms.

References

[1] Y. Avigal, Diamond and Related Materials, 1, 216 (1992).

[2] P. A. Denning, H. Shiomi, D. A. Stevenson and N. M. Johnson, Thin Solid Films, 212, 63 (1992).

[3] V. Bortolani, N. H. March and M. P. Tosi (eds), *Interaction of Atoms and Molecules with Solid Surfaces*, Plenum Press, New York, 1990.

[4] T. Halicioglu, Surf. Sci., 285, 259 (1993).

[5] J. Tersoff, Phys. Rev., B 39, 5566 (1989).

[6] J. Tersoff, Phys. Rev. Lett., 64, 1757 (1990).

[7] H. Balamane, T. Halicioglu and W. A. Tiller, Phys. Rev., B, 46, 2250 (1992).

[8] T. Halicioglu, Surf. Sci., 259, L714 (1991).

[9] P. Ascarelli, S. Fontana, G. Cossu, E. Cappelli and N. Nistico, Diamond and Related Materials, 1, 211 (1992).

[10] J. W. Kim, Y. J. Baik and K. Y. Eun, Diamond and Related Materials, 1, 200 (1992).

Table 1. Calculated binding energies of carbon atoms adsorbed on a (2×1) reconstructed Si(100) surface for varying surface coverages. Lower case letters in the third column indicate occupied sites by carbon adatoms corresponding to Figure 1.

Structure Number	Coverage θ	Occupied Sites	ϕ_x (eV)
1	1	a through p	−5.9661
2	3/4	a,b,c,d,e,f,g,h,i,j,k,l	−6.2075
3	3/4	a,b,c,e,f,h,i,k,l,n,o,p	−6.0917
4	3/4	a,b,c,e,f,g,i,j,k,m,n,o	−5.7938
5	1/2	a,b,c,d,e,f,g,h	−6.3492
6	1/2	a,b,c,d,i,j,k,l	−6.1551
7	1/2	a,c,f,h,i,k,n,p	−5.9866
8	1/2	a,c,e,g,i,k,m,o	−5.9695
9	1/2	a,b,e,f,i,j,m,n	−5.9676
10	1/4	a,b,c,d	−6.3722
11	1/4	a,b,e,f	−6.3529
12	1/4	a,c,i,k	−6.0613
13	1/4	a,e,i,m	−5.9694
14	1/8	a,b	−6.2997
15	1/8	a,e	−6.2524
16	1/8	b,c	−6.2261
17	1/8	a,c	−6.2071
18	1/8	b,g	−6.1970
19	1/8	a,f	−6.1577
20	1/8	a,i	−6.0631
21	1/16	a	−6.1935

Figure Captions

1. Top view of a relaxed Si(100) surface. Letters *a* through *p* indicate low energy sites for adsorbed carbon atoms. Identical low energy sites on this surface are indicated by letters *a* through *p* which are located near the top position of a second layer Si atom. Silicon atoms in first, second and third layers from the top are represented by large open circles, solid circles and small open circles, respectively.

2. Variation in binding energies for carbon atoms as a function of the surface coverage.

3. Top (a) and side (b) views of the energetically most favorable structure for C_3 deposited on a Si(100) surface. Silicon atoms located in the first and second layers were represented by large and small open circles, respectively, while carbom atoms are designated by solid circles. The C-C bond distance and bond angle are given in units of Å and degrees.

4. Top (a) and side (b) views of the energetically most favorable structure for C_4 deposited on a Si(100) surface. (Symbols are described in the caption of Figure 3).

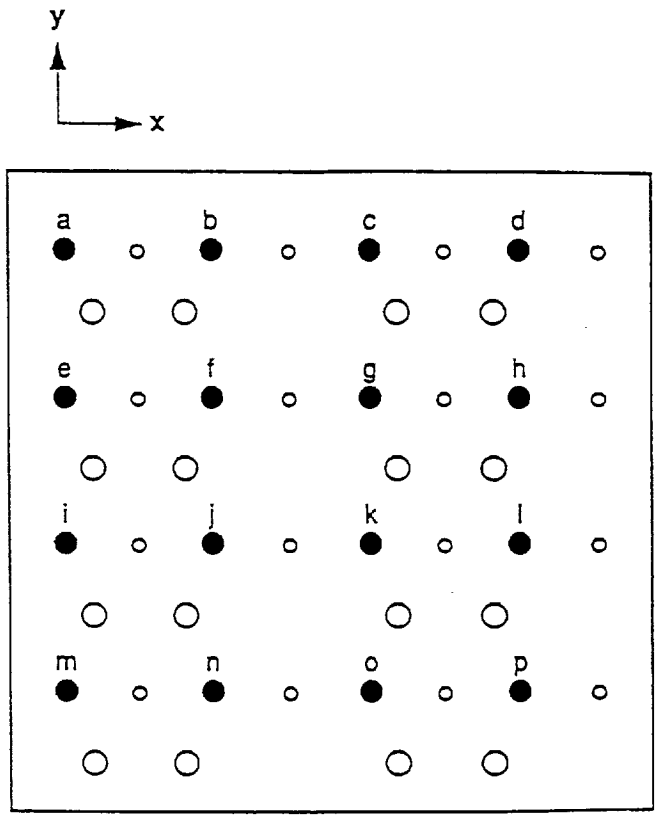

Figure 1

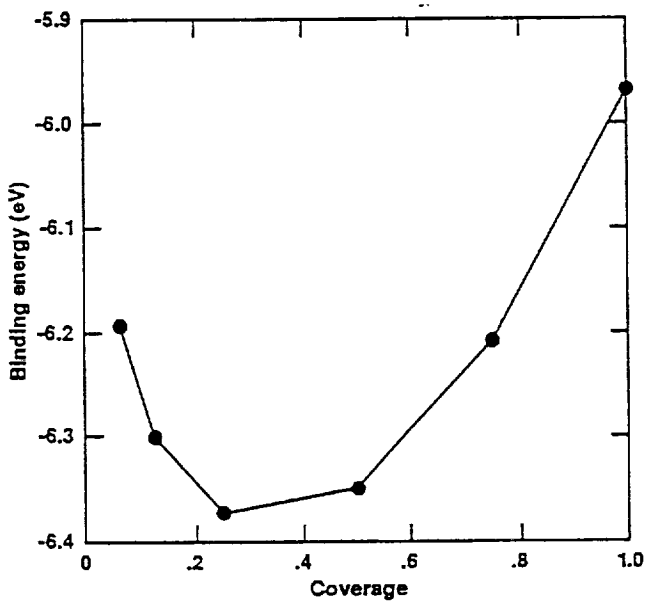

Figure 2

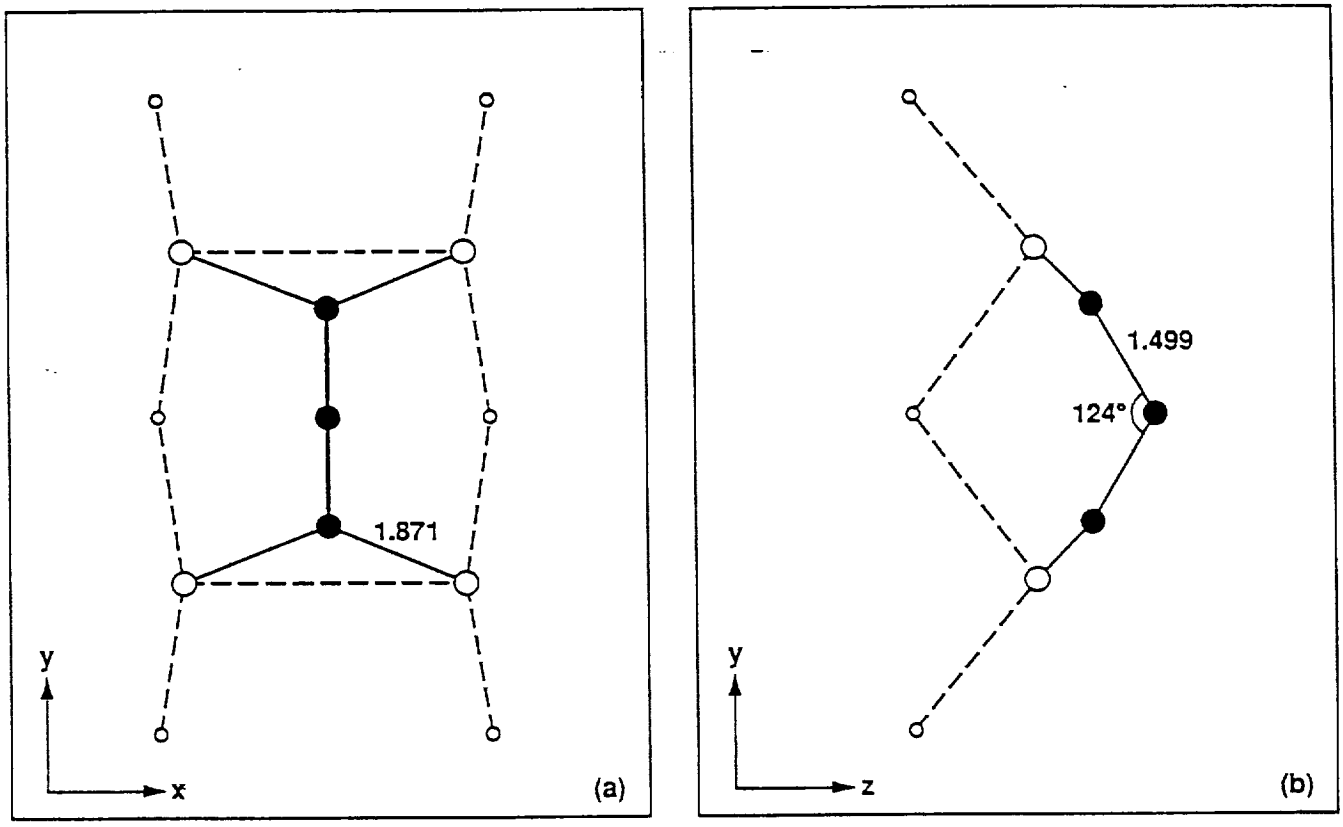

Figure 3

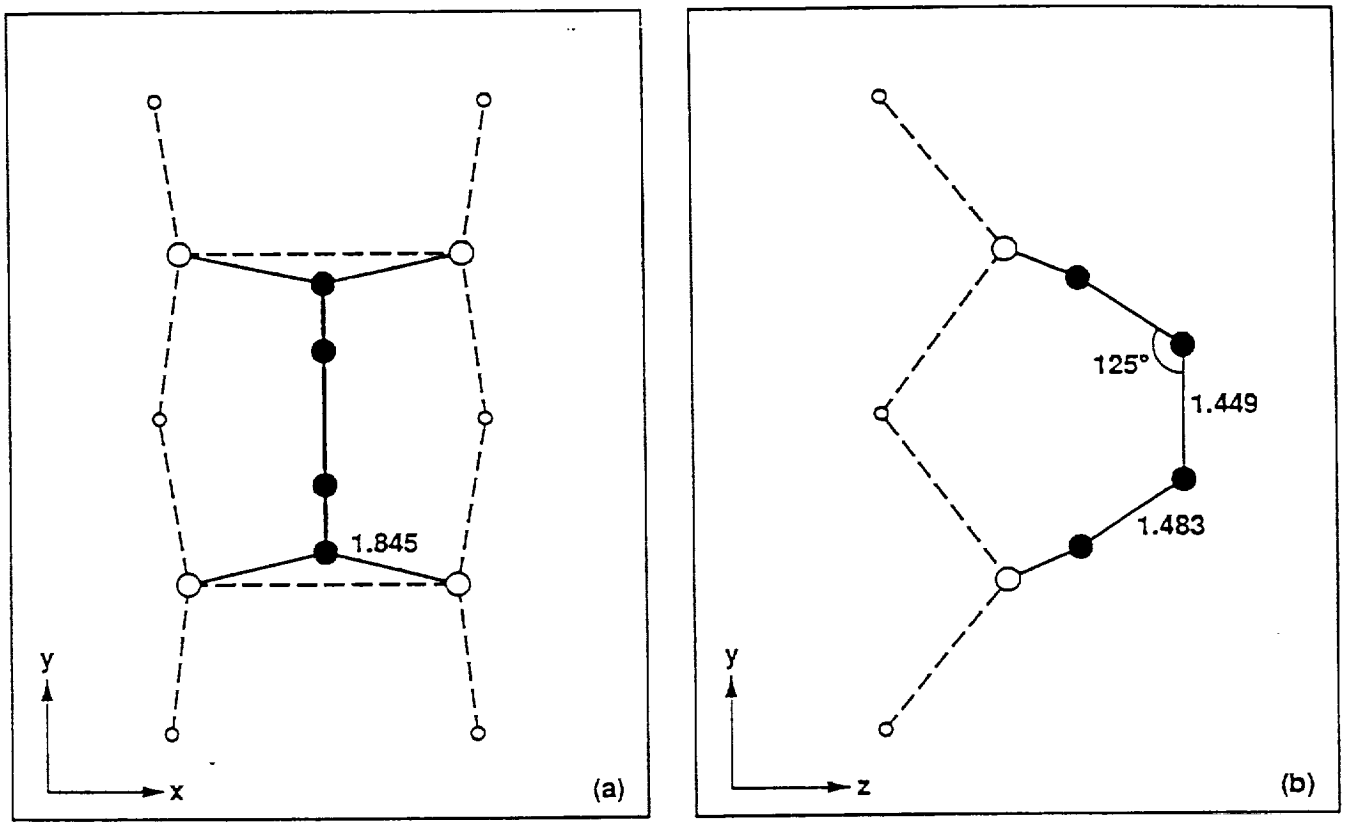

Figure 4

APPENDIX III:

Strain Dependence of Binding Energies for Carbon Adatoms on the Si(100) Surface

Strain is an important factor in the physics of surfaces, based on both theory and experiments. Many surface related processes (such as surface segregation, formation of orientational domains, surface diffusion, nucleation and surface reconstruction) are influenced by strains applied to the system [1-3]. Strain produces changes in the surface atomic arrangements which, in turn, alter surface energetics. The importance of the strain effect on diamond nucleation on Si substrates has been demonstrated recently by Lin, et al. [4].

In this investigation calculations were carried out to estimate strain dependence of the binding energy of a carbon atom deposited on a (2×1) reconstructed Si(100) surface. Binding energies were calculated for C atoms positioned on the lowest and second lowest energy sites of a reconstructed Si(100) surface as a function of applied external strain. In a recent study, energy- and structure-dependent properties of these favorable binding sites have been documented in detail [5].

In this work all calculations were carried out using a static method based on an energy minimization technique. To calculate energies, a model potential function developed by Tersoff, specifically for systems containing Si and C atoms, was employed [6,7]. In all cases, the binding energy, ϕ_b, for a carbon adatom was calculated as $\phi_b = E_a - E^o$, where E^o denotes the total equilibrated energy of the system of N particles with clean exposed surfaces, and E_a is the total relaxed energy of the same system with a carbon adatom deposited on the surface.

Calculations were performed considering a system with a (100) surface generated as an abrupt termination of the bulk silicon in the diamond cubic structure. This system, then, was fully equilibrated pro-

ducing a (2×1) reconstruction pattern at the exposed surfaces. The lattice constant for the bulk Si (for the unstrained case) was taken as 5.43 Å, corresponding to the equilibrium volume of Si calculated by the Tersoff function. All calculations were carried out considering a 4×4 computational cell made of a slab of 16 atomic layers, each containing 16 Si atoms. This cell size has already been shown to be adequate for the convergence of the surface energy [5]. Using a cartesian coordinate system the (100) surface was positioned parallel to the x-y plane with the y-direction running perpendicular to the Si-dimers (see Figure 1). Throughout this study, periodic boundary conditions were imposed on the system in x- and y-directions (parallel to the exposed surface) in order to eliminate the edge effect.

A top view of the two lowest energy sites for C atoms adsorbed on a (2×1) reconstructed Si(100) surface are shown schematically in Figure 1. The lowest energy site at this surface is indicated by letter A. It is located near the top position of a second layer Si atom. The second lowest energy site, on the other hand, is at the bridge site between two top layer Si atoms forming the dimer. This second lowest energy site is denoted by letter B.

Uniaxial compressive and tensile strains were applied to the substrate in either x- or y-directions by factorizing the corresponding atomic coordinates (as well as corresponding periodic boundaries) by a desired percentage amount denoted by f_s. While, f_s=1 represents the unstrained case, values of f_s larger (and smaller) than 1 correspond to systems under tension (and compression). In all cases binding energies were obtained using the values for E_a as well as E^o that were estimated considering sytems equilibrated under desired strain conditions. Calculations were performed for different f_s values varying between 0.98

to 1.02. These values correspond to a 2% margin for strains varying from compressive to tensile limits. Within these limits, atomic separations for all cases were found to remain uniformly spaced in the direction of the applied strain after relaxation.

Variations in the calculated binding energies as a function of the strain factor f_s are shown in Figure 2 for the lowest and second lowest binding sites. For the lowest energy site (at the near top position of a second layer Si atom) calculations produced a small dependence for ϕ_b on strains applied in the x-direction. The binding energy decreases with increasing tension in the x-direction, producing a relatively small negative slope (about -1.38 eV per f_s). However, a large dependence of ϕ_b was found on strain applied in the y-direction. The variation in the binding energy in this case has a positive slope and a compressive strain favors the binding. The slope at f_s=1 is positive and it was calculated as 10.46 eV per f_s.

The second lowest energy site for an adsorbed carbon atom on a (2×1) reconstructed Si(100) surface, is located at the bridge position above the mid-point of a Si dimer. The binding energy for a C adatom at this site displays a small dependence on the applied strain. In this case a tensile strain in the x-direction promotes binding, as in the previous case, with a small negative slope of -0.776 at f_s=1. In the y-direction, however, the effect of the strain on ϕ_b is rather small. At f_s=1, it produced a positive slope of only 0.4369 per f_s.

Present results indicate that strain effect on the binding energy of a carbon atom adsorbed on a reconstructed Si(100) surface may be important. In general, strains applied in the directions parallel and perpendicular to surface Si-dimers, were found to produce opposing effects on binding energies. For both the lowest and the second lowest binding

sites, calculated binding energies were found to increase slowly with increased compression applied in the direction parallel to the surface Si-dimers. In the case of strains applied in the direction perpendicular to Si-dimers, however, binding energy values decreased (i.e., the bond strength increased) with increasing compression. In this case the variation in the binding energy was estimated to be quite significant for the lowest energy site, while for the second lowest site the change in the binding energy was found to be rather small.

It was shown in this investigation (based on purely energetic considerations) that binding of carbon atoms on a reconstructed Si(100) surface is energetically favored for increasing compressive strains applied parallel to the Si-dimers direction. This outcome may generate important implications in the very early stages of the nucleation process in C atom deposition experiments.

References

[1] M. B. Webb, F. K. Men, B. S. Schwartzentruber, R. Kariotis and M. G. Lagally, Surf. Sci., 242, 23 (1991).

[2] R. D. Meade and D. Vanderbilt, Phys. Rev. B, 40, 3905 (1989).

[3] F. K. Men, W. E. Packard and M. B. Webb, Phys. Rev. Lett., 61, 2469 (1988).

[4] S. J. Lin, S. L. Lee, J. Hwang, C. S. Chang and H. Y. Wen, Appl. Phys. Lett., 60, 1559 (1992).

[5] T. Halicioglu, Surf. Sci., 285, 259 (1993).

[6] J. Tersoff, Phys. Rev., B 39, 5566 (1989).

[7] J. Tersoff, Phys. Rev. Lett., 64, 1757 (1990).

Figure Captions:

1. A schematic top view of the two lowest energy sites for C adatoms on a (2×1) reconstructed Si(100) surface. The lowest and second lowest binding sites are denoted by letters A and B, respectively. Dimerized Si atoms of the top layer are shown by squares. Si atoms in the second and third layers are indicated by ◇ and ×.

2. Variations in the calculated binding energies for C atoms deposited in the lowest and second lowest sites on the Si(100) surface, as a function of f_s.

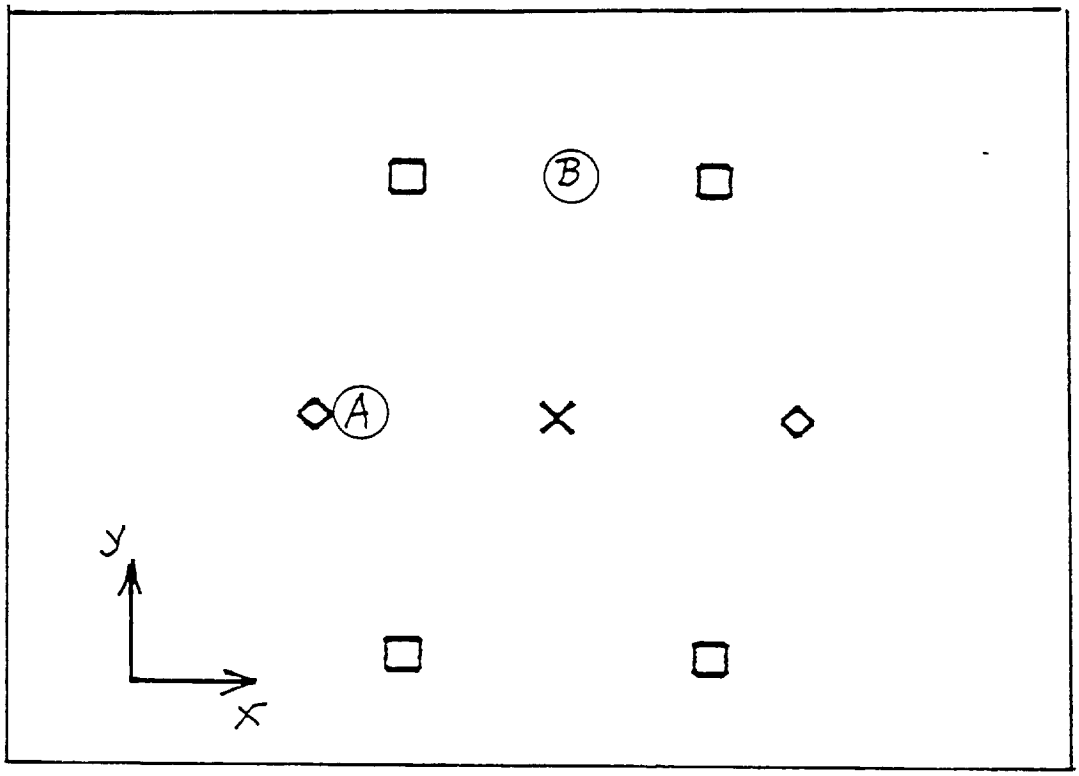

Figure 1

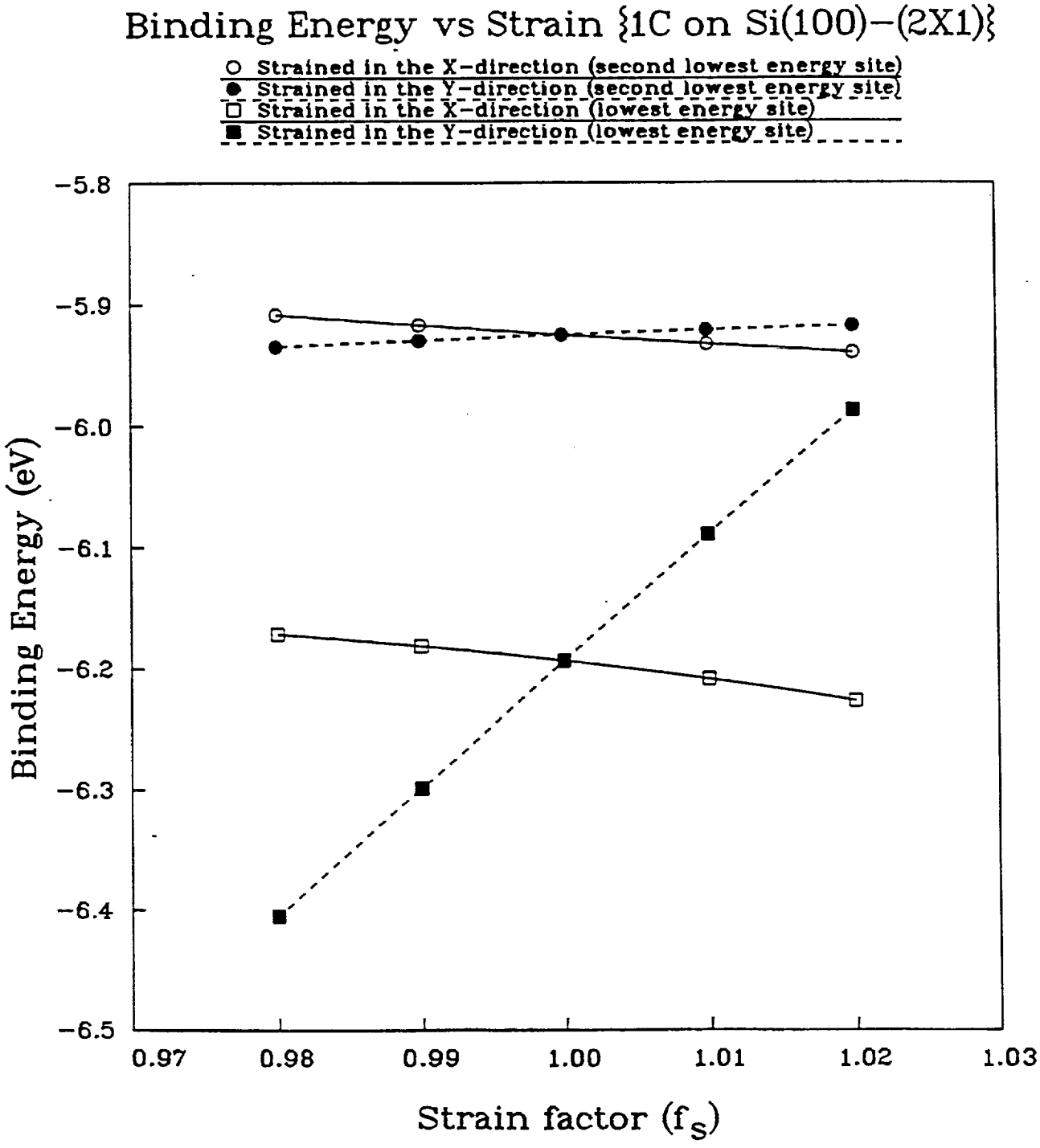
Binding Energy vs Strain {1C on Si(100)−(2X1)}
Strained in the X-direction (second lowest energy site)
Strained in the Y-direction (second lowest energy site)
Strained in the X-direction (lowest energy site)
Strained in the Y-direction (lowest energy site)
−5.8
−5.9
−6.0
−6.1
−6.2
−6.3
−6.4
−6.5
Binding Energy (eV)
0.97
0.98
0.99
1.00
1.01
1.02
1.03
Strain factor (f_s)

Figure 2